

# Fractional flux periodicity in tori made of square lattice

K. Sasaki<sup>\*)</sup>, Y. Kawazoe and R. Saito<sup>1</sup>

*Institute for Materials Research, Tohoku University, Sendai 980-8577, Japan*

<sup>1</sup>*Department of Physics, Tohoku University and CREST, JST, Sendai 980-8578, Japan*

We present a study on fractional flux periodicity of the ground state in planar systems made from a square lattice whose boundary is compacted into a torus. The ground-state energy and persistent currents show a fractional period of the fundamental unit of magnetic flux depending on the twist around the torus axis. We discuss the possible relationship between the twist and genus of a torus.

## §1. Introduction

The Aharonov-Bohm effect<sup>1)</sup> shows that a single electron wave function has a fundamental unit of magnetic flux  $\Phi_0 = 2\pi/e$ , where  $-e$  is the electron charge <sup>\*\*)</sup> . The electrical and magnetic properties of materials are governed by many electrons, and each constituent has the above-mentioned periodicity. However, the fundamental flux period of a material is not always  $\Phi_0$ . For example, superconducting materials exhibit a period of  $\Phi_0/2$ , which can be understood by charge doubling due to the Cooper pair formation. This is clear if one imagines that a fundamental particle (or quasiparticle) has a  $-2e$  charge due to attractive interaction, and that the fundamental flux period of a material is equal to that of the quasiparticle ( $2\pi/2e$ ) in the system.

In Fig. 1, we depict schematic diagrams of typical experimental settings for the Aharonov-Bohm effect. Consider an electron going over and under a very long impenetrable cylinder, denoted as a black circle in Fig. 1(a). In the cylinder there is a magnetic field parallel to the cylinder axis, taken as normal to the plane of the figure. The probability of finding this electron in the interference region depends on the magnetic field  $\Phi$  and the interference pattern having period  $\Phi_0$ . When an electron is placed in a ring pierced by a magnetic flux  $\Phi$  as shown in Fig. 1(b), a current  $I$  defined by differentiating the ground state energy with respect to the magnetic flux, appears and is expected to have the flux periodicity  $\Phi_0$ . Actual mesoscopic rings contain many electrons, and non vanishing currents, known as persistent currents,<sup>2)-4)</sup> are also expected.

Although the ground state in mesoscopic rings consists of many electrons, because each electron has the flux periodicity  $\Phi_0$  one might think the flux periodicity of the systems is the same as the flux periodicity of the constituent electron. In this paper, we present an example in which the fundamental flux period of the ground-state does not coincide with the flux periodicity of the constituent particle. We will

---

<sup>\*)</sup> E-mail address: sasaken@imr.edu

<sup>\*\*)</sup>  We will use the units of  $\hbar = c = 1$ .

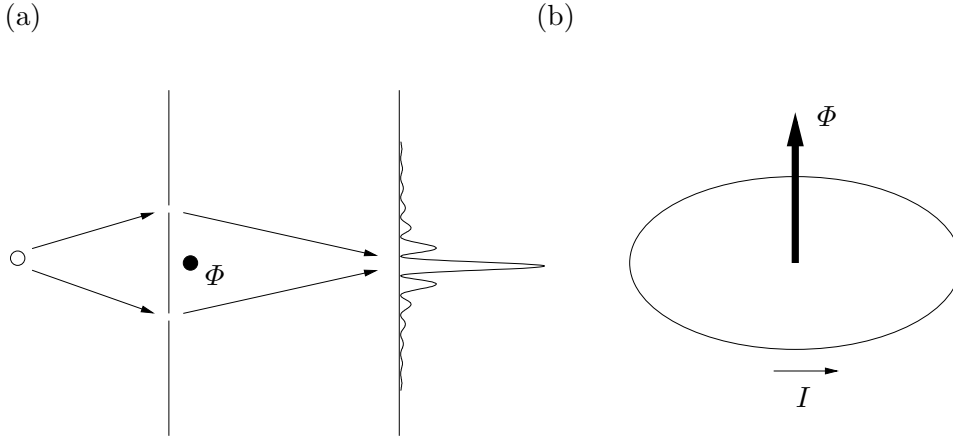


Fig. 1. Schematic diagram of (a) an Aharonov-Bohm experiment and (b) Aharonov-Bohm ring. In (a), electrons are emitted from the source region, denoted by the empty circle, and produce the interference pattern. In (b), one-dimensional ring is pierced by a magnetic field and exhibits a persistent current.

show that a fractional flux periodicity  $(\Phi_0/2, \Phi_0/3, \dots)$  can be realized in planar systems of a square lattice whose geometry is a torus. To analyze the flux periodicity of the systems, we consider the ground state energy and persistent currents. These are considered suitable for examining the flux periodicity of the ground state since they are regarded as the Aharonov-Bohm effect in solid state systems.<sup>4)</sup> In the previous paper,<sup>5)</sup> we showed a typical example of a fractional periodicity in the Aharonov-Bohm effect. Here, we extend the theory in general cases and give detailed derivation of the results.

This paper is organized as follows. In Section 2, we obtain an explicit formula for the ground state energy and plot it for different lattice structures, showing the fractional flux periodicity numerically. In Section 3, we examine the persistent currents and prove fractional flux periodicity noting that the characteristic features of the ground state energy can be understood in terms of the twist-induced gauge field. In Section 4, we give a discussion and summary of our results. Throughout this paper we ignore electron spin and the effect of finite temperature.

## §2. Ground state energy

The lattice structure of a torus is specified by two vectors: the chiral, given by  $C_h = NT_x + MT_y$ , and the translational, given by  $T_w = PT_x + QT_y$ , where  $N, M, P$  and  $Q$  are integers and  $T_a$  ( $a = x, y$ ) is the unit vector of the square lattice in the direction of  $x$  and  $y$  where we define  $x$  and  $y$  in the two dimensional map (see Fig. 3(b)). We borrow this terminology from the carbon nanotube context.<sup>6)</sup> Here,  $C_h$  ( $T_w$ ) characterizes the lattice structure around (along) the tube axis. It is useful to rewrite  $T_a$  in terms of the chiral and translational vectors as

$$\begin{pmatrix} T_x \\ T_y \end{pmatrix} = \frac{1}{N_s} \begin{pmatrix} Q & -M \\ -P & N \end{pmatrix} \begin{pmatrix} C_h \\ T_w \end{pmatrix}, \quad (1)$$

where we define  $N_s \equiv NQ - MP$ , and  $|N_s|$  corresponds to the number of square lattices on the surface of the torus given by  $C_h \times T_w = N_s(T_x \times T_y)$ . In this paper, we take the  $x$  axis in the direction of  $C_h$  ( $M = 0$ ), and denote  $P = \delta N$  to describe the *twist* around the tube axis. Then,  $C_h \cdot T_w = \delta N N a^2$  where  $a(= |T_x| = |T_y|)$  is the lattice constant. We depict an example of twisted torus in Fig. 2, in which all sites are connected by a line consisting nearest-neighbor bond. Fig. 3(a) shows

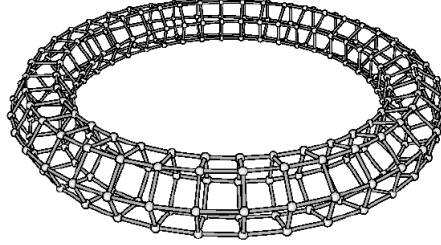


Fig. 2. Lattice structure of a twisted torus. The lattice configuration is given by  $N = 6$ ,  $Q = 40$  and  $\delta N = 1$ .

an illustration of the twisted torus. A torus can be unrolled to a parallelogram sheet as shown in Fig. 3(b). In the figure, the two lines extending upward from ‘u’ and downward from ‘d’ and having the same ‘ $x$ ’ at the junction are not joined for a twisted torus, as shown in the inset of Fig. 3(a). There are  $\delta N$  square lattices between the two lines.

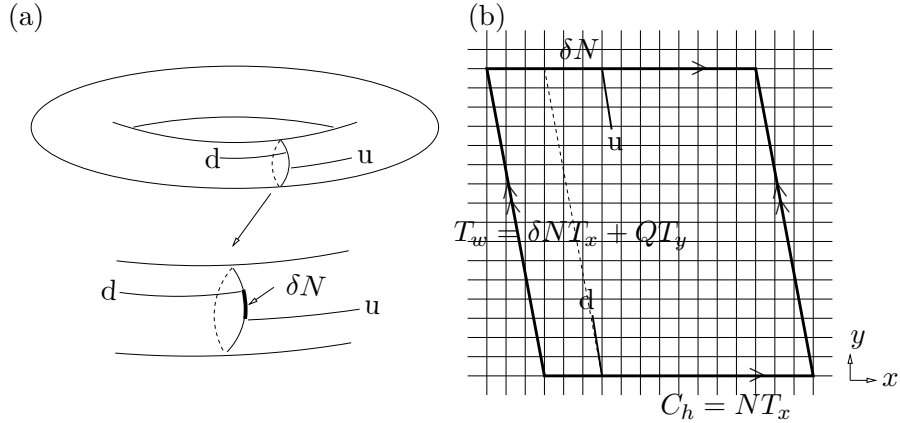


Fig. 3. Schematic diagram of (a) a twisted torus (upper) and the extension around a cross section (lower), and (b) its net diagram. It is convenient to consider a parallelogram sheet of square lattice as the net diagram of a twisted torus, where the chiral and translational vectors become the vectors at the sides of the parallelogram. The lattice configuration is given by  $N = 14$ ,  $Q = 16$  and  $\delta N = -3$ .

The quantum mechanical behavior of conducting electrons on a square lattice is modeled by the nearest-neighbor tight-binding Hamiltonian:

$$\mathcal{H} = -t \sum_i \sum_{a=x,y} a_{i+a}^\dagger e^{-ieA^{\text{ex}} \cdot T_a} a_i + h.c., \quad (2)$$

where  $t$  is the hopping integral,  $A^{\text{ex}}$  is a constant external gauge field (vector potential), and  $a_i$  and  $a_i^\dagger$  are canonical annihilation-creation operators of the electrons at site  $i$  that satisfy the anti-commutation relation  $\{a_i, a_j^\dagger\} = \delta_{ij}$ . We diagonalize  $\mathcal{H}$  in terms of the Bloch basis parametrized by wave vector  $k$  and obtain  $\mathcal{H} = \sum_k E(k - eA^{\text{ex}}) a_k^\dagger a_k$ , where  $a_k \equiv \frac{1}{\sqrt{|N_s|}} \sum_i e^{ik \cdot r_i} a_i$  is the annihilation operator of the Bloch orbital. The energy eigenvalue of the Hamiltonian  $E(k - eA^{\text{ex}})$  is given by,

$$E(k - eA^{\text{ex}}) = -2t\Re \left( \sum_{a=x,y} e^{i(k - eA^{\text{ex}}) \cdot T_a} \right). \quad (3)$$

The Bloch wave vector satisfies the periodic boundary condition for  $C_h$  and  $T_w$  through which the geometrical (or topological) information of a torus, such as the twist, is entered into the energy eigenvalue. We decompose wave vector  $k$  as  $\mu_1 k_1 + \mu_2 k_2$ , where  $k_1$  and  $k_2$  are defined by

$$C_h \cdot k_1 = 2\pi, \quad C_h \cdot k_2 = 0, \quad T_w \cdot k_1 = 0 \quad \text{and} \quad T_w \cdot k_2 = 2\pi. \quad (4)$$

Here,  $k_1$  and  $k_2$  can be rewritten in terms of the reciprocal lattice vectors  $K_x$  and  $K_y$  as

$$k_1 = \frac{1}{N_s}(QK_x - \delta N K_y), \quad k_2 = \frac{1}{N_s}(N K_y), \quad (5)$$

where the reciprocal lattice vectors are defined by  $K_a \cdot T_b = 2\pi\delta_{ab}$  with  $a, b = x, y$ . Components  $\mu_1$  and  $\mu_2$  are quantum numbers (integers) and define the Brillouin zone as

$$\left[ -\frac{N}{2} \right] + 1 \leq \mu_1 \leq \left[ \frac{N}{2} \right], \quad \left[ -\frac{Q}{2} \right] + 1 \leq \mu_2 \leq \left[ \frac{Q}{2} \right], \quad (6)$$

where  $[n]$  indicates the maximum integer smaller than  $n$ .

We point out that the wave vector shifts according to the twist of a torus. For example, in the absence of twist ( $\delta N = 0$ ),  $k_1$  and  $k_2$  are proportional to  $K_x$  and  $K_y$ , respectively and perpendicular to each other; otherwise, they are not. The shift of the wave vector plays an important role when we consider the ground state configuration, which we discuss below. Here we rewrite Eq.(3) by means of Eqs.(1) (with  $M = 0$  and  $P = \delta N$ ) and (4) as

$$E(k - eA^{\text{ex}}) = -2t \left\{ \cos \left( \frac{2\pi\mu_1}{N} \right) + \cos \left( \frac{2\pi(\mu_2 - \frac{\delta N}{N}\mu_1) - eA^{\text{ex}} \cdot T_w}{Q} \right) \right\}, \quad (7)$$

where we assume  $A^{\text{ex}} \cdot C_h = 0$ , and  $A^{\text{ex}} \cdot T_w$  corresponds to the Aharonov-Bohm flux penetrating the center of the torus. The ground state is defined as the state for which all electronic states below (above) the Fermi surface are occupied (empty). We consider a half-filling system and set the Fermi energy  $E_F = 0$ . We define the Fermi line in the two dimensional Brillouin zone, within which all states are occupied as the solution of  $E(k) = 0$ , forming a square as shown in Fig. 4(a). The side of the square (or Fermi line) is denoted by  $k^\pm$  and  $k_\pm$ . Each energy eigenstate is labeled

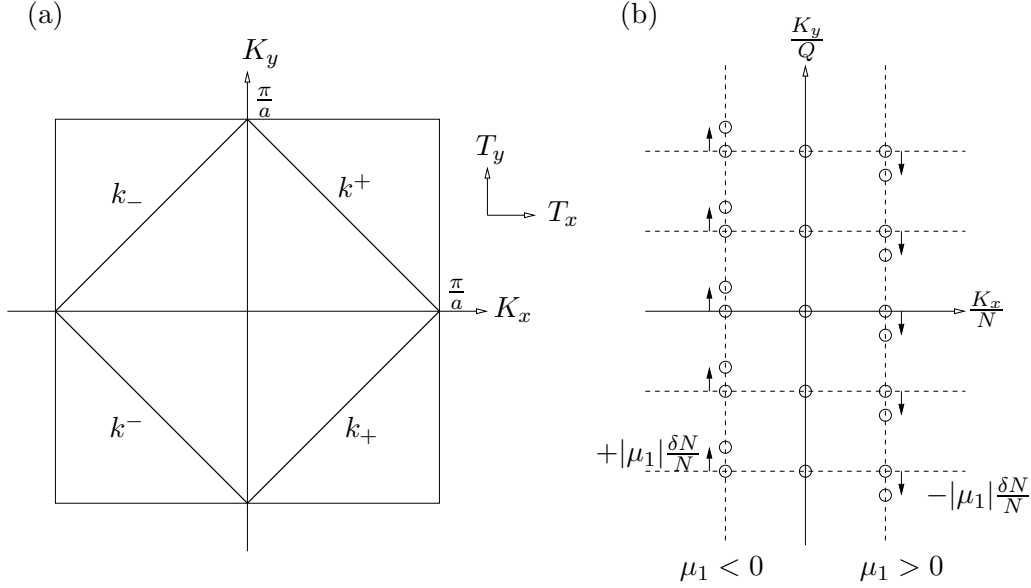


Fig. 4. Brillouin zone and Fermi lines in momentum space (a), and schematic diagram of the wave vector shifting due to the twist around the axis (b). There are two factors we should take into account to define the ground state. The first factor is the effect of the twist. Compared with the ground-state configuration in an untwisted torus, Eq.(5) indicates that the location of the energy eigenstates shifts depending on twist  $\delta N$  and on the electron motion around the axis ( $\mu_1$ ). This shift is illustrated in (b), where we denote the Bloch states as circles and depict several states of positive  $\mu_1$ , negative  $\mu_1$  and  $\mu_1 = 0$ . In the absence of twist, all states are located at mesh line crossings. When twist is present, the states shift depending on their  $\mu_1$  and  $\delta N/N$ . The second factor is the external gauge field. The external gauge field can shift the wave vector, however, the shift is independent of electron motion contrary to the case where twist is present.

by  $\mu_1$  and  $\mu_2$  and thus we can specify the occupied states by  $\mu_1$  and  $\mu_2$  explicitly. In fact the region inside the Fermi line is defined as

$$-\pi \leq \frac{2\pi\mu_1}{N} + \frac{2\pi(\mu_2 - \frac{\delta N}{N}\mu_1) - eA^{\text{ex}} \cdot T_w}{Q} \leq \pi, \quad (8)$$

$$-\pi \leq \frac{2\pi\mu_1}{N} - \frac{2\pi(\mu_2 - \frac{\delta N}{N}\mu_1) - eA^{\text{ex}} \cdot T_w}{Q} \leq \pi, \quad (9)$$

where we note that the Fermi lines satisfy  $k^\pm \cdot (T_x + T_y) = \pm\pi$  and  $k_\pm \cdot (T_x - T_y) = \pm\pi$ , and Eqs.(8) and (9) can be rewritten as

$$k^- \cdot (T_x + T_y) \leq (k - eA) \cdot (T_x + T_y) \leq k^+ \cdot (T_x + T_y), \quad (10)$$

$$k_- \cdot (T_x - T_y) \leq (k - eA) \cdot (T_x - T_y) \leq k_+ \cdot (T_x - T_y). \quad (11)$$

For a fixed value of  $\mu_1$ , we obtain the following region of  $\mu_2$ , in which all states are occupied by electrons:

$$\left[ -Q \left( \frac{1}{2} - \frac{\mu_1}{N} \right) + \frac{\delta N}{N} \mu_1 + N_\Phi \right] + 1 \leq \mu_2 \leq \left[ Q \left( \frac{1}{2} - \frac{\mu_1}{N} \right) + \frac{\delta N}{N} \mu_1 + N_\Phi \right], \quad (12)$$

for  $\mu_1 \geq 0$ , and

$$\left[ -Q \left( \frac{1}{2} + \frac{\mu_1}{N} \right) + \frac{\delta N}{N} \mu_1 + N_\Phi \right] + 1 \leq \mu_2 \leq \left[ Q \left( \frac{1}{2} + \frac{\mu_1}{N} \right) + \frac{\delta N}{N} \mu_1 + N_\Phi \right], \quad (13)$$

for  $\mu_1 \leq 0$ , respectively. Here, we set  $A^{\text{ex}} \cdot T_w = \Phi$  and define the number of Aharonov-Bohm flux  $N_\Phi \equiv \Phi/\Phi_0$ . The ground-state energy is therefore

$$E_0(\Phi) = \sum_{\mu_1 = \left[ -\frac{N}{2} \right] + 1}^{\left[ \frac{N}{2} \right]} \sum_{\mu_2 = \left[ -Q \left( \frac{1}{2} - \frac{|\mu_1|}{N} \right) + \frac{\delta N}{N} \mu_1 + N_\Phi \right] + 1}^{\left[ Q \left( \frac{1}{2} - \frac{|\mu_1|}{N} \right) + \frac{\delta N}{N} \mu_1 + N_\Phi \right]} E(k - eA^{\text{ex}}). \quad (14)$$

This is the explicit mathematical expression for the ground state energy of a twisted torus.

Here, we plot  $E_0(\Phi)/4t$  for different  $N$ ,  $\delta N$  and  $Q$  as a function of  $N_\Phi$ , and observe the characteristics of the results. Fig. 5 shows the dependence of the ground state energy on  $\delta N$ , where we fix  $N = 80$  and  $Q = 160$  and vary the twist as  $\delta N = 1, 20, 40$ . The flux periodicity is determined to be  $\Phi_0/2$  for  $\delta N = 1$  (solid line) and  $\delta N = 40$  (dashed line), and  $\Phi_0/4$  for  $\delta N = 20$  (dotted line). We note that the fractional flux periodicity of the dashed and dotted lines corresponds to the lattice structure of  $\delta N/N$ . In addition to observing fractional flux periodicity, we see that the solid line is smooth at  $N_\Phi = 0$  for example, when compared with the other two lines.

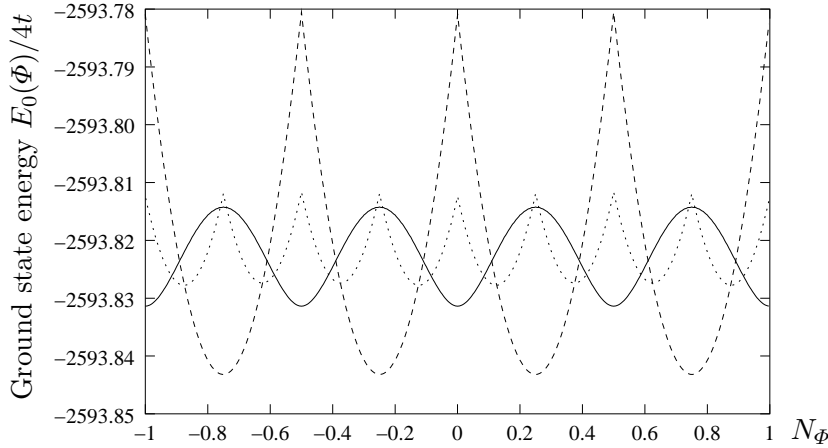


Fig. 5. Ground state energy as a function of flux. We fix  $N = 80$  and  $Q = 160$ , then plot for  $\delta N = 1, 20, 40$  to examine the dependence of the ground-state energy on twist. We observe a flux periodicity of  $\Phi_0/2$  for  $\delta N = 1$  (solid line) and  $\delta N = 40$  (dashed line) and  $\Phi_0/4$  for  $\delta N = 20$  (dotted line). For the untwisted torus ( $N = 40$ ,  $Q = 160$  and  $\delta N = 0$ ), refer to Fig. 9.

Next we examine the dependence of the ground state energy on the diameter of the tube  $N$ . Figs. 6, 7 and 8 show the ground state energy with fixed  $Q = 160$  and  $\delta N = 20$  while varying  $N = 40, 80, 160$ . Observing the flux periodicity of the samples, they appear precisely to be periodic in Figs. 6, 7 and 8 with a period of

$\Phi_0/2$  in Fig. 6 and  $\Phi_0/4$  in Fig. 7. They are not periodic, however, due to a small modulation in the ground state energy. This is manifest in Fig. 8. This modulation can be thought of as a finite size correction scaled as  $\mathcal{O}(N/Q)$  (see Appendix A).

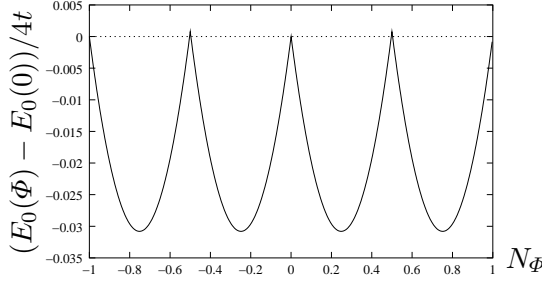


Fig. 6. Ground state energy for  $N = 40$ ,  $Q = 160$  and  $\delta N = 20$ . We plot  $(E_0(\Phi) - E_0(0))/4t$  where  $E_0(0)/4t = -1296.892$ .

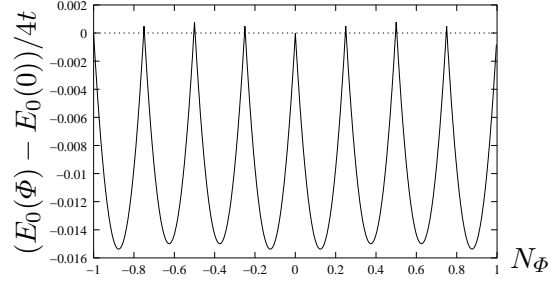


Fig. 7. Ground state energy for  $N = 80$ ,  $Q = 160$  and  $\delta N = 20$ . We plot  $(E_0(\Phi) - E_0(0))/4t$  where  $E_0(0)/4t = -2593.812$ .

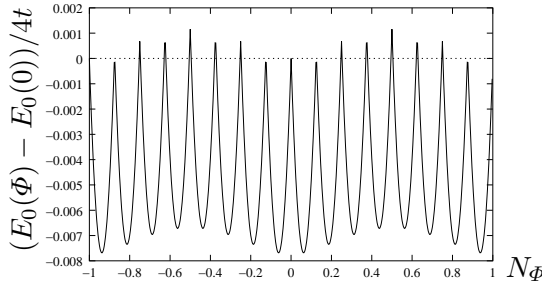


Fig. 8. Ground state energy for  $N = 160$ ,  $Q = 160$  and  $\delta N = 20$ . We plot  $(E_0(\Phi) - E_0(0))/4t$  where  $E_0(0)/4t = -5187.640$ .

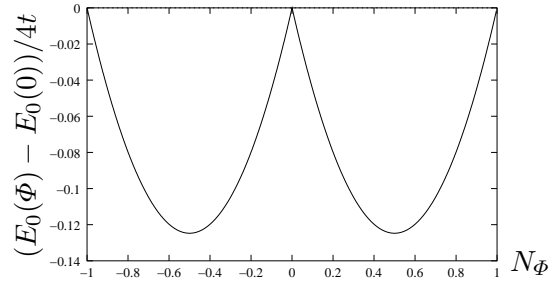


Fig. 9. Ground state energy for  $N = 40$ ,  $Q = 160$  and  $\delta N = 0$ . We plot  $(E_0(\Phi) - E_0(0))/4t$  where  $E_0(0)/4t = -1296.83$ .

Finally, we observe the dependence of the ground state energy on  $Q$  shown in Figs. 9,

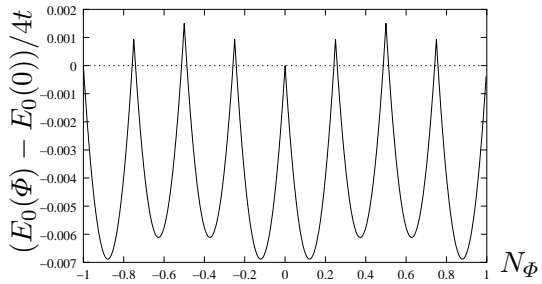


Fig. 10. Ground state energy for  $N = 40$ ,  $Q = 170$  and  $\delta N = 0$ . We plot  $(E_0(\Phi) - E_0(0))/4t$  where  $E_0(0)/4t = -1377.965$ .

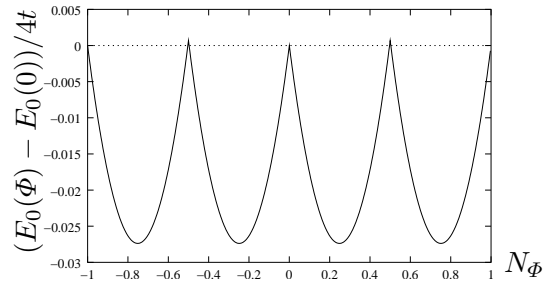


Fig. 11. Ground state energy for  $N = 40$ ,  $Q = 180$  and  $\delta N = 0$ . We plot  $(E_0(\Phi) - E_0(0))/4t$  where  $E_0(0)/4t = -1459.008$ .

10 and 11. Here, we note that all previous examples have had the common feature of  $Q$  as a multiple of  $N$ . Fig. 9 shows the standard flux periodicity  $\Phi_0$ . In Fig. 11, however, we have a periodicity of  $\Phi_0/2$  even in the absence of twist.

It is important to mention that the amplitude of the oscillation of  $E_0(\Phi)$  depends much on  $N$ ,  $Q$  and  $\delta N$ . We will discuss the dependence of amplitude on them in the next section.

### §3. Persistent currents and interpretation of the numerical results

In the previous section, we presented a formula for the ground state energy. By plotting the energy for different values of  $N$ ,  $\delta N$  and  $Q$ , we found that some tori exhibit a fractional flux periodicity. In this section, we will present an analytical results that demonstrate and prove fractional flux periodicity for a twisted torus in terms of the persistent currents. By so doing, we clarify the relationship between the lattice structure and flux periodicity.

Persistent current is defined by differentiating the ground state energy with respect to the magnetic flux  $\Phi$ :<sup>4)</sup>

$$I_{\text{pc}}(\Phi) = -\frac{\partial E_0(\Phi)}{\partial \Phi}. \quad (15)$$

Because  $E_0(\Phi)$  consists of many energy dispersion relations as specified by  $\mu_1$  (hereafter referred to as  $\mu_1$ -th energy band), we can write

$$E_0(\Phi) = \sum_{\mu_1 = [-\frac{N}{2}] + 1}^{[\frac{N}{2}]} E(\mu_1, \Phi) \quad (16)$$

where  $E(\mu_1, \Phi)$  is the ground state energy of  $\mu_1$ -th energy band and is the sum of the energy at  $\mu_2$ -th  $k$  points which satisfy Eqs.(12) and (13):

$$E(\mu_1, \Phi) \equiv \sum_{\mu_2 = [-Q(\frac{1}{2} - \frac{|\mu_1|}{N}) + \frac{\delta N}{N}\mu_1 + N\Phi] + 1}^{[Q(\frac{1}{2} - \frac{|\mu_1|}{N}) + \frac{\delta N}{N}\mu_1 + N\Phi]} E(\mu_1 k_1 + \mu_2 k_2 - eA^{\text{ex}}). \quad (17)$$

Hence, the persistent current can also be decomposed into the current of each energy band as

$$I_{\text{pc}}(\Phi) = \sum_{\mu_1 = [-\frac{N}{2}] + 1}^{[\frac{N}{2}]} I(\mu_1, \Phi), \quad \text{where } I(\mu_1, \Phi) \equiv -\frac{\partial E(\mu_1, \Phi)}{\partial \Phi}. \quad (18)$$

To calculate the persistent currents in long systems with  $|T_w| \gg |C_h|$  (or  $Q \gg N$ ), we do not need to sum over the energy eigenvalue of the valence electrons but just calculate the Fermi velocity of the energy band. Because, when we vary the magnetic field, the change of the ground state energy is almost determined by the change of the energy eigenvalue of electrons near the Fermi level and that of the energy eigenvalues deep in energy bands cancel to one another. In terms of Fermi velocity, the amplitude of  $I(\mu_1, \Phi)$  (the persistent current for the  $\mu_1$ -th energy band) is well approximated



by<sup>4)</sup>

$$I(\mu_1) = \frac{ev_F(\mu_1)}{|T_w|}, \quad (19)$$

where  $|T_w|$  is the system length and  $v_F(\mu_1)$  denotes the Fermi velocity of the  $\mu_1$ -th energy band. The proof of this approximation is given in Appendix A. We fix  $\mu_1$  and expand Eq.(7) on  $\mu_2$  around the Fermi level, then we obtain the energy dispersion relation of the  $\mu_1$ -th energy band as

$$\mathcal{H}_{\mu_1} = v_F(\mu_1)p_2 - \frac{1}{2m(\mu_1)}p_2^2 + \mathcal{O}(p_2^3). \quad (20)$$

where  $p_2(\equiv \mu_2 k_2)$  denotes the momentum along the axis. Notice that we can include  $eA^{\text{ex}} \cdot T_w$  by replacing  $p_2$  with the covariant momentum, and that Eq.(20) represents the case for  $\mu_2 > 0$ . For  $\mu_2 < 0$ , the energy dispersion relation is defined by  $-\mathcal{H}_{\mu_1}$  up to  $\mathcal{O}(p_2)$ . The coefficient of  $p_2$  gives the Fermi velocity and the coefficient of  $p_2^2$  gives the effective mass if  $v_F(\mu_1) = 0$ . They are then defined respectively as

$$v_F(\mu_1) = 2ta \left| \sin \left( \frac{2\pi\mu_1}{N} \right) \right|, \quad \frac{1}{2m(\mu_1)} = ta^2 \cos \left( \frac{2\pi\mu_1}{N} \right). \quad (21)$$

First we consider persistent currents in an untwisted torus ( $\delta N = 0$ ). In this case, all energy bands yield the same function for the persistent current, that is, a saw-tooth curve as a function of  $\Phi$  with the same zero points (the flux for which the amplitude of the current vanishes) but with different amplitudes<sup>\*)</sup>. In fact, the amplitude of the total current is given by a summation of all amplitudes:

$$I_{\text{tot}} = \sum_{\mu_1 = [-\frac{N}{2}] + 1}^{[\frac{N}{2}]} I(\mu_1) = \frac{2eta}{|T_w|} \cot \frac{\pi}{N}. \quad (22)$$

Persistent current  $I_{\text{pc}}$  in the torus is given by  $I_{\text{tot}}$  multiplied by  $\phi/\pi$  ( $\phi \equiv 2\pi(\Phi/\Phi_0)$ ). The linear relation between  $\Phi$  and the persistent currents has a periodicity of  $\Phi_0$ , and we then have a saw-tooth current:

$$I_{\text{pc}}^{\delta N=0}(\phi) = I_{\text{tot}} \frac{2}{\pi} \sum_{n=1}^{\infty} (-1)^{n+1} \frac{\sin(n\phi)}{n}. \quad (23)$$

The saw-tooth persistent current is a characteristic of the non-interacting theories at zero temperature. Each saw-tooth curve loses its sharpness due to disorder, or at finite temperature.<sup>7)</sup> We note here, and in all subsequent discussions, that we are implicitly assuming the amplitude of the persistent current vanishes at  $\phi = 0$ . Generally, the zero amplitude points depend on the total number of electrons in the system and may be  $\phi = 2\pi j$  or  $\phi = 2\pi j + \pi$  where  $j$  is an integer (Appendix A). As for the flux periodicity, the zero amplitude position does not affect the results. We note also that the persistent current corresponding to the ground state energy shown in Fig. 9 can be approximated by Eq.(23) with the replacement  $\phi \rightarrow \phi - \pi$ .

<sup>\*)</sup> Here, we implicitly assume  $Q$  is a multiple of  $N$  (see the comments at the end of this section).

Next, we analyze a twisted torus ( $\delta N \neq 0$ ). To understand the effect of twist on the persistent currents, we introduce gauge field  $A^{\text{twist}}$ . In terms of  $A^{\text{twist}}$ , the second term of the right hand side of Eq.(7) can be rewritten as

$$\cos \left( \frac{2\pi\mu_2 - (eA^{\text{ex}} + \mu_1 A^{\text{twist}}) \cdot T_w}{Q} \right), \quad (24)$$

where we define  $A^{\text{twist}} \cdot C_h \equiv 0$  and  $A^{\text{twist}} \cdot T_w \equiv 2\pi\delta N/N$ . Like  $A^{\text{ex}}$ ,  $A^{\text{twist}}$  can shift the wave vector. However, the shift depends on the twist ( $\delta N/N$ ) and the wave vector around the tube axis ( $\mu_1 k_1$ ). Because of this, coupling between  $A^{\text{twist}}$  and the conducting electron preserves the time-reversal symmetry of the whole system. This is contrasted with the broken time-reversal symmetry of  $A^{\text{ex}}$ . The twist behaves as an extra gauge field and shifts the wave vector along the axis direction, so that the zero points of the persistent current also shift.<sup>8)</sup> As a result, in order to calculate the total current, we must sum the saw-tooth curves that have different zero points and different amplitudes, all of which depend on  $\mu_1$ . Then we have

$$I_{\text{pc}}^{\delta N}(\phi) = \frac{2eta}{|T_w|} I_N^{\delta N}(\phi), \quad (25)$$

where  $I_N^{\delta N}(\phi)$  is expressed as

$$\begin{aligned} I_N^{\delta N}(\phi) &= \frac{2}{\pi} \sum_{\mu_1 = [-\frac{N}{2}] + 1}^{[\frac{N}{2}]} \sum_{n=1}^{\infty} (-1)^{n+1} \frac{\sin(n(\phi - 2\pi\mu_1 \frac{\delta N}{N}))}{n} \left| \sin\left(\frac{2\pi\mu_1}{N}\right) \right| \\ &= \frac{1}{\pi} \sum_{n=1}^{\infty} (-1)^{n+1} \frac{\sin(n\phi)}{n} (1 + \cos(n\pi\delta N)) \left( \frac{2 \sin(\frac{2\pi}{N})}{\cos(\frac{2\pi n\delta N}{N}) - \cos(\frac{2\pi}{N})} \right). \end{aligned} \quad (26)$$

Persistent currents exhibit the following characteristic depending on an even or odd number of  $\delta N$ . Term  $1 + \cos(\pi n\delta N)$  in Eq.(26) vanishes if  $n\delta N$  is an odd number or is equal to 2 for other cases. Then Eq.(26) reduces to

$$I_N^{\delta N}(\phi) = \begin{cases} -\frac{1}{\pi} \sum_{n=1}^{\infty} \frac{\sin(2n\phi)}{n} C_n^o & \text{for } \delta N = \text{odd}, \\ \frac{2}{\pi} \sum_{n=1}^{\infty} \frac{(-1)^{n+1} \sin(n\phi)}{n} C_n^e & \text{for } \delta N = \text{even}, \end{cases} \quad (27)$$

where  $C_n^o$  and  $C_n^e$  are given

$$C_n^o = \frac{2 \sin(\frac{2\pi}{N})}{\cos(\frac{4\pi n\delta N}{N}) - \cos(\frac{2\pi}{N})}, \quad C_n^e = \frac{2 \sin(\frac{2\pi}{N})}{\cos(\frac{2\pi n\delta N}{N}) - \cos(\frac{2\pi}{N})}. \quad (28)$$

The difference in periodicity for  $\phi$  is clear because  $\sin(2n\phi)$  has a period one half the fundamental unit of magnetic flux, or  $\Phi_0/2$ . The solid line ( $\delta N = 1$ ) in Fig. 5 is an example of  $\delta N = \text{odd}$  showing the one-half flux periodicity. This conclusion is valid

for any number of  $N$ , but a *fundamental* flux periodicity for a current demonstrates a more interesting behavior for a specific combination of  $N$  and  $\delta N$ .

Let us consider a particular structure for  $\delta N/N = 1/3$  where  $\delta N$  is an even number. In this case, the fundamental period of  $C_n^e$  is 3, i.e.,  $C_{n+3}^e = C_n^e$ . When  $N \gg 1$ , we have  $C_1^e = C_2^e \approx -8\pi/3N$  and  $C_3^e \approx 2N/\pi$ . We then obtain

$$\begin{aligned} I_N^{\delta N}(\Phi) &= \frac{2}{\pi} \sum_{n=0}^{\infty} \sum_{m=1}^3 (-1)^{3n+m+1} \frac{\sin((3n+m)\phi)}{3n+m} C_m^e \\ &= \frac{2}{3\pi} \sum_{n=1}^{\infty} (-1)^{n+1} \frac{\sin(3n\phi)}{n} C_3^e + \mathcal{O}(1/N) \\ &\approx \frac{2N}{\pi^2} \phi \quad \text{for } N \gg 1, \end{aligned} \quad (29)$$

where in the last line of Eq.(29) we assume  $-\pi/3 < \phi < \pi/3$ . The fundamental flux period of Eq.(29) becomes  $\Phi_0/3$ . It should be noted that this argument can be applied to other twisted structures. For instance, when  $\delta N/N = 1/Z$  ( $1/Z = 1/4, 1/5, \dots$ ), we obtain another fractional period of  $\Phi_0/Z$ . To our knowledge, this is the first time a fractional periodicity for a twisted boundary condition has been found. We note that the total persistent currents are still saw-tooth curves as expected from the non-interacting theories. The ground state energy corresponding to  $Z = 2$  and  $Z = 4$  is plotted in Fig. 5 as dashed and dotted lines.

Finally, let us remark that the amplitude of the current exhibits a nontrivial dependence on  $\Phi$  when  $N \rightarrow \infty$  with a fixed value of  $\delta N$ . If we divide  $I_N^{\delta N}(\phi)$  by  $N$  and take the limit of  $N \rightarrow \infty$ , we then have

$$\lim_{N \rightarrow \infty} \frac{I_N^{\delta N}(\phi)}{N} = \begin{cases} -\frac{2}{\pi^2} \sum_{n=1}^{\infty} \frac{\sin(2n\phi)}{n} \frac{1}{1 - 4n^2\delta N^2} & \text{for } \delta N = \text{odd}, \\ \frac{4}{\pi^2} \sum_{n=1}^{\infty} (-1)^{n+1} \frac{\sin(n\phi)}{n} \frac{1}{1 - n^2\delta N^2} & \text{for } \delta N = \text{even}. \end{cases} \quad (30)$$

When  $\delta N \gg 1$ , we sum  $n$  in the above equations and obtain

$$\lim_{N \rightarrow \infty} \frac{I_N^{\delta N}(\phi)}{N} = \begin{cases} \frac{(\pi - 2\phi)(\pi^2 - (2\phi - \pi)^2)}{24\pi^2\delta N^2} & \text{for } 0 \leq \phi \leq \pi \text{ and } \delta N = \text{odd}, \\ -\frac{\phi(\pi^2 - \phi^2)}{3\pi^2\delta N^2} & \text{for } -\pi \leq \phi \leq \pi \text{ and } \delta N = \text{even}, \end{cases} \quad (31)$$

where we have used the following mathematical formula:

$$\sum_{n=1}^{\infty} \frac{\sin(n\phi)}{n^3} = \frac{(\pi - \phi)(\pi^2 - (\phi - \pi)^2)}{12} \quad \text{for } 0 \leq \phi \leq 2\pi, \quad (32)$$

$$\sum_{n=1}^{\infty} (-1)^{n+1} \frac{\sin(n\phi)}{n^3} = \frac{\phi(\pi^2 - \phi^2)}{12} \quad \text{for } -\pi \leq \phi \leq \pi. \quad (33)$$

In Fig. 12, we plot the persistent currents of Eq.(31) for an even and odd number of  $\delta N$  as a function of  $\phi$ . It should be noted that the persistent currents are not standard saw-tooth curves even though we are considering non-interacting electrons, and the functional shape of Eq.(31) for  $\delta N$  is an odd number similar to  $\sin(2\phi)$  but not identical (see Fig. 12). The solid line ( $\delta N = 1 = \text{odd}$ ) in Fig. 5 may be regarded as an example of Eq.(30) and shows a smooth curve as a function of  $\Phi$ .

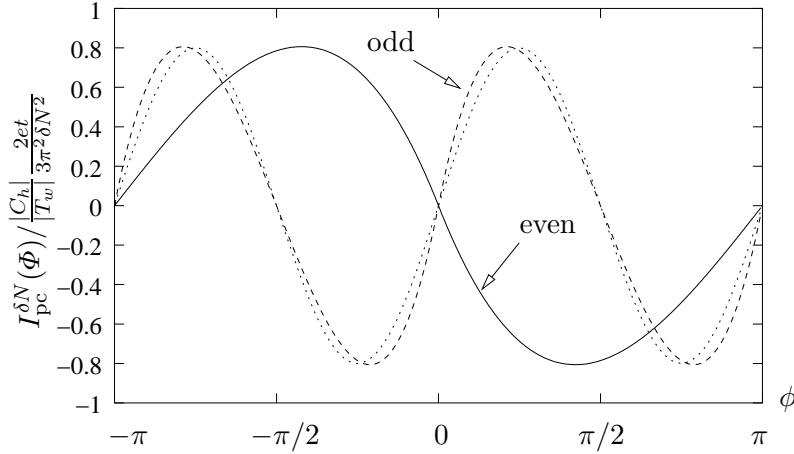


Fig. 12. Persistent currents as  $N \rightarrow \infty$  (Eq.31) for an even (solid line) and an odd (dashed line) number of  $\delta N$ . We multiply 2 (16) for an even (odd) number case. We also plot  $0.8\sin(2\phi)$  (dotted line) for comparison.

Summarizing our results: (1) A fundamental flux period of the ground-state can be generally fractional as  $\Phi_0/Z$ , depending on the ratio of twist  $\delta N$  to  $N$ , although we do not assume any interaction that can form a quasiparticle of charge  $Ze$ ; (2) As  $N \rightarrow \infty$  with fixed value  $\delta N (\gg 1)$ , the currents are not standard saw-tooth as is normally expected from non-interacting theories; and (3) To observe fractional periodicity, it is essential that the system contain many electrons,  $N \gg 1$  and  $Q \gg N$ , indicating a kind of “many body” effect.

The primary factor in these results is the Fermi surface structure of the square lattice. It appears that many energy bands cross the Fermi level when we roll a planar sheet into a cylinder, and electrons near the Fermi level in each energy band contribute to the persistent currents which interfere with one another due to the twist. This point can be made clear by comparing a square lattice with a honeycomb lattice (which possesses only two distinct Fermi points). In this case, we can observe at most a  $\Phi_0/2$  periodicity.<sup>8)</sup>

Finally we briefly discuss the dependence of persistent currents on the value of  $Q$ . So far we implicitly assumed that  $Q$  is a multiple of  $N$ . For a general  $Q$  and a general structure (different chiral and translational vectors), the persistent currents are not as simple<sup>8)</sup> as the results obtained in this study. For example, when the remainder of  $Q/N$  is an odd number, the one-half periodicity may emerge even in the absence of twist. Furthermore, another fractional period may appear for a specific value of  $Q$ . This complication can be understood by Eq.(12). For  $\mu_1 \geq 0$ ,

we have the occupied states

$$\left[ -Q \left( \frac{1}{2} - \frac{\mu_1}{N} \right) + \frac{\delta N}{N} \mu_1 + N_\Phi \right] + 1 \leq \mu_2 \leq \left[ Q \left( \frac{1}{2} - \frac{\mu_1}{N} \right) + \frac{\delta N}{N} \mu_1 + N_\Phi \right]. \quad (34)$$

The term  $(\delta N/N)\mu_1 + N_\Phi$  clearly indicates that the shift of the wave vector is in one direction. Suppose  $Q$  is an even number and we set  $Q = nN + \delta Q$  ( $n$  is an integer). Then the above inequality reduces to

$$- \left( \frac{Q}{2} - n\mu_1 \right) + \left[ \frac{\delta N + \delta Q}{N} \mu_1 + N_\Phi \right] + 1 \leq \mu_2 \leq \left( \frac{Q}{2} - n\mu_1 \right) + \left[ \frac{\delta N - \delta Q}{N} \mu_1 + N_\Phi \right], \quad (35)$$

which shows an asymmetry of the left and right Fermi point in the  $\mu_1$ -th energy band because of the  $(\delta Q/N)\mu_1$  term. Moreover, this term cannot be regarded as the gauge field presented in this paper.

#### §4. Discussion and summary

In this paper, we presented an example in which the fundamental flux period of the ground-state does not coincide with the flux periodicity of the constituent particle. We showed that a fractional flux periodicity  $(\Phi_0/2, \Phi_0/3, \dots)$  can be realized in twisted tori made of square lattice. Table I summarizes the relationship between the lattice structure and flux periodicity of persistent currents, derived in this study. First, we classify the tori into two types depending on whether or not  $\delta Q$  is zero, where  $\delta Q$  is defined as the remainder of  $Q/N$ . As we have discussed in the text, for  $\delta Q \neq 0$ , we have no clear classification of the relationship. When  $Q$  is a multiple of  $N$ , we classify the relationship in terms of the twist-induced gauge field. For untwisted tori, we show the single-electron flux periodicity  $\Phi_0$  and for twisted tori we have Eq.(27).

Here, we discuss some possible extensions of our results. Because we have observed a fractional periodicity in the ground state, one may ask the following question: “Is it possible that the persistent currents show multiple periods such as  $2\Phi_0$  or  $3\Phi_0$  as a fundamental period?” To answer this question, we consider higher genus materials ( $g$ : number of holes), the ground state of which exhibit  $g\Phi_0$  periodicity depending on the genus ( $g = 2, 3, \dots$ ).<sup>9)</sup> A planar system comprising a finite number of square lattices is an example of higher genus material. We note that the conducting electrons in that case are also assumed to be non-interacting and have a single electron charge. Moreover, other examples are known where the charge of a quasiparticle itself becomes fractional. The quasiparticle in the quantum Hall effect has fractional charge  $e/3$ <sup>10)</sup> and there is a model containing a fractional  $e/2$  charged soliton in 1+1 dimensions.<sup>11)</sup>

Lattice Structure and Flux Periodicity		
$\delta Q$	$\delta N$	Period (in units of $\Phi_0$ )
$\delta Q = 0$	$\delta N = 0$	1
	$\delta N \neq 0$	$1/Z$ for $\delta N/N = 1/Z$

Table I. Flux periodicity of (large) tori. For  $\delta Q \neq 0$ , we do not obtain any clear relationship between the lattice structure and flux periodicity.

Those systems might exhibit  $3\Phi_0$  or  $2\Phi_0$  periodicity in the ground state, respectively. However, examples of fractional periods other than  $\Phi_0/2$  (which may correspond to a multiple charge  $e \rightarrow 3e, 4e, \dots$ ) have thus far not been found as far as we know.

Considering the possibility that the system exhibits flux periodicity such as  $(2/3)\Phi_0, (2/5)\Phi_0$ , when we consider a torus with  $g = 1$  such a periodicity seems impossible. However, for higher genus materials ( $g \geq 2$ ), there is still a chance for a fundamental flux period of  $(g/Z)\Phi_0$ , where  $Z$  is an integer. Such a periodicity may exist when the twist and genus can be simultaneously defined for a higher genus material, although we have no idea if one can define twist in higher genus materials.

In summary, we have examined the flux periodicity of the ground state of conducting electron on a torus of square lattice. We found that the persistent currents and the ground-state energy of the systems show fractional periods of the fundamental unit of magnetic flux ( $\Phi_0/2, \Phi_0/3, \dots$ ) depending on twist  $\delta N$  and  $N$ . Furthermore, for the case of  $N \rightarrow \infty$  with a fixed value of  $\delta N (\gg 1)$ , the persistent currents are not standard saw-tooth curves as expected from the non-interacting theories at zero temperature.

### Acknowledgments

K. S. is supported by a fellowship of the 21st Century COE Program of the International Center of Research and Education for Materials of Tohoku University. R. S. acknowledges a Grant-in-Aid (No. 13440091) from the Ministry of Education, Japan.

### Appendix A

#### —— Persistent current and Fermi velocity ——

We prove that the amplitude of the persistent current is approximated by Eq.(19) for a long system ( $Q \gg N$ ). For simplicity, let us first consider an untwisted torus and fix  $Q$  as an even numbered multiple of  $N$ . Then

$$\left[ -Q \left( \frac{1}{2} - \frac{|\mu_1|}{N} \right) + N_\Phi \right] = -Q \left( \frac{1}{2} - \frac{|\mu_1|}{N} \right), \quad (\text{A}\cdot 1)$$

holds for  $0 \leq N_\Phi < 1$  because the right hand side of Eq.(A·1) is an integer. It follows from Eqs.(7),(17),(18) and (A·1) that for  $0 \leq N_\Phi < 1$

$$\begin{aligned} I(\mu_1, \Phi) &= \sum_{\mu_2 = -Q(\frac{1}{2} - \frac{|\mu_1|}{N}) + 1}^{Q(\frac{1}{2} - \frac{|\mu_1|}{N})} \frac{2t}{\Phi_0} \frac{2\pi}{Q} \sin \left( \frac{2\pi(\mu_2 - N_\Phi)}{Q} \right) \\ &= \frac{ev_F(\mu_1)}{|T_w|} (2N_\Phi - 1) + \frac{e}{2m(\mu_1)} \frac{2\pi(2N_\Phi - 1)}{|T_w|^2} + \mathcal{O}(Q^{-3}), \end{aligned} \quad (\text{A}\cdot 2)$$

where we have used Eq.(21) in the last line. This shows that the amplitude of the persistent current of  $\mu_1$ -th energy band is approximated by Eq.(19) and a correction

on the order of  $I(\mu_1)\mathcal{O}(N/Q)$  can be ignored for long systems of  $Q \gg N$ . Similarly, for an odd number of  $Q$  up to  $\mathcal{O}(Q^{-1})$  we have

$$I(\mu_1, \Phi) = \frac{ev_F(\mu_1)}{|T_w|} 2N_\Phi \quad \text{for } -\frac{1}{2} \leq N_\Phi < \frac{1}{2}. \quad (\text{A}\cdot 3)$$

### References

- 1) Y. Aharonov and D. Bohm, Phys. Rev. **115** (1959) 485.
- 2) M. Büttiker, Y. Imry, and R. Landauer, Phys. Lett. A **96** (1983) 365; R. Landauer and M. Büttiker, Phys. Rev. Lett. **54** (1985) 2049.
- 3) L.P. Lévy, G. Dolan, J. Dunsmuir, and H. Bouchiat, Phys. Rev. Lett. **64** (1990) 2074; V. Chandrasekhar, R.A. Webb, M.J. Brady, M.B. Ketchen, W.J. Gallagher, and A. Kleinsasser, Phys. Rev. Lett. **67** (1991) 3578; D. Mailly, C. Chapelier, and A. Benoit, Phys. Rev. Lett. **70** (1993) 2020.
- 4) Y. Imry, *Introduction to Mesoscopic Physics* (Oxford University Press, New York, 1997).
- 5) K. Sasaki, Y. Kawazoe, and R. Saito, arXiv:cond-mat/0401597.
- 6) R. Saito, G. Dresselhaus, and M.S. Dresselhaus, *Physical Properties of Carbon Nanotubes* (Imperial College Press, London, 1998) Chapter 3.
- 7) M. Büttiker, Phys. Rev. B **32** (1985) 1846; H.F. Cheung, Y. Gefen, E.K. Riedel, and W.H. Shih, Phys. Rev. B **37** (1988) 6050.
- 8) K. Sasaki and Y. Kawazoe, arXiv:cond-mat/0307339.
- 9) K. Sasaki, Y. Kawazoe, and R. Saito, Phys. Lett. A **321** (2004) 369.
- 10) D.C. Tsui, H.L. Stormer, and A.C. Gossard, Phys. Rev. Lett. **48** (1982) 1559; R.B. Laughlin, Phys. Rev. Lett. **50** (1983) 1395.
- 11) R. Jackiw and C. Rebbi, Phys. Rev. D **13** (1976) 3398.